A NEW GENERATION OF J INTEGRAL FRACTURE SPECIMENS FOR LARGE-SCALE BRIDGING PROBLEMS

B. F. Sørensen

[1]*Section of Composites and Materials Mechanics, Department of Wind Energy, Technical University of Denmark, Risø Campus, Frederiksborgvej 399, 4000 Roskilde, Denmark*
**bsqr@dtu.dk*

Keywords: fracture mechanics, fiber composites, crack bridging, J integral

Abstract
Mode I, Mode II and mixed mode fracture mechanics test specimens, well suited for the characterization of large-scale bridging in terms of traction-separation laws using a J integral approach, are presented. They all allow stable crack growth. J integral equations are obtained in closed analytical form and are independent of details of the traction-separation law representing the bridging. This allows the determination of the traction-separation laws without the further numerical modeling of the test specimens. Differences between J integral fracture specimens and traditional linear-elastic fracture specimens are highlighted.

1 Introduction

Some fiber composites develop a crack bridging zone during interlaminar cracking (delamination) or intralaminar cracking (splitting). Crack bridging is usually considered as being a desirable phenomenon, since it leads to increasing fracture resistance and enhanced damage tolerance [1]. The size of the bridging zone can be large in comparison with the so-called K-dominant region, i.e., the region near the crack tip where the stress field follows the singular crack tip stress field of linear-elastic fracture mechanics (LEFM). When the bridging zone extends in the wake of the crack outside the K-dominant zone (large-scale bridging, LSB), as shown in Figure 1, the deformation of the specimen outside the K-dominant zone influences the development of the crack bridging and thus the crack growth. LEFM criteria for crack propagation, such as critical values of stress intensity factors or energy release rates, are then insufficient to characterize crack growth since they do not account for the energy dissipation in the bridging zone [2, 3]. The mechanical response of the bridging zone can be described in terms of traction-separation laws, so-called bridging laws or cohesive laws [3].
It is major challenge to determine traction-separation laws for real materials. A widely used approach is to perform fracture experiments and record relations between load and displacement of the specimens. Next, a numerical model (e.g., incremental finite element models) is made of the specimen. The model includes a cohesive zone in which traction-separation laws can be prescribed. Idealized traction-separation laws having a pre-determined shape, e.g., a bi-linear traction-separation relation, are used. Key parameters such as the peak traction value and steady-state fracture resistance (area under the traction-separation curve) are identified by iterative guessing, e.g., by conducting several simulations using different trial traction-separation parameters; the parameter set that gives the closest agreement with the experimental data is then taken to represent the true traction-separation law. While such an

approach is feasible and gives very satisfactory results [4-6], it requires new simulations for each new material being tested. It is thus a more complicated procedure than the analysis of fracture toughness for LEFM specimens, for which standard solutions are made once and for all and tabulated in hand books [7].
The aim of the present study is to present a general approach for the determination of traction-separation laws for LSB problems, an approach that does not require finite element simulation of the specimen for each new material or interface tested. The proposed approach is based on the utilization of the path-independent J integral [8]. The J integral approach for determination of Mode I traction-separation laws was first proposed by Li and Ward [9], while J integral specimens for LSB problems were first considered by Suo *et al.* [2]. A J integral approach for the determination of mixed mode traction-separation laws was proposed by Sørensen and Kirkegaard [10]. In the present paper we briefly summarize the J integral approach and focus on specimen for which (a) the crack growth is stable, so that experimental data can be obtained for the whole separation process and thus enables the determination of the complete traction-separation law and (b) the J integral solution can be obtained in closed analytical form, independent of the details of the traction-separation laws (whish are initially unknown). Full filling (b) enables the analysis of the J integral fracture mechanics test specimens as standard solutions similar to the LEFM hand book solutions for the stress intensity factors.

Figure 1. Photo of a glass fibre composite experiencing large-scale crack bridging.

2 J integral analyses of a bridged crack

First we will briefly review the salient feature of the J integral approach for the determination of traction-separation laws. Consider a fracture process zone consisting of a sharp crack and a bridging zone. Evaluating the J integral along a local path just around the fracture process zone (bridging zone and crack tip) give during cracking [10]:

$$J_R = J_{loc} = \int_0^{\Delta_n^*} T_n \, d\Delta_n + \int_0^{\Delta_t^*} T_t \, d\Delta_t + J_0 \,, \tag{1}$$

where J_R is the fracture resistance, T_n and T_t, denote the normal and shear tractions, respectively, Δ_n and Δ_t are the normal and tangential crack opening displacements, Δ_n^* is the end-opening, Δ_t^* is the end-sliding, see Fig. 2, and J_0 is the crack tip fracture energy. Equation (1) can be given a physical interpretation: The J integral equals the sum of the work

per unit area of the normal and shear tractions at the end of the bridging zone and the energy dissipation at the crack tip (the crack tip fracture energy).

In general, both T_n and T_t are functions of both Δ_n and Δ_t. Furthermore, it is assumed that the critical crack openings exist, Δ_n^0 and Δ_t^0, beyond which the tractions vanish. Assuming that the tractions are derivable from a potential function, the mixed mode traction-separation relations can be obtained as [10]

$$T_n\left(\Delta_n^*,\Delta_t^*\right)=\frac{\partial J_R\left(\Delta_n^*,\Delta_t^*\right)}{\partial\Delta_n^*}\qquad T_t\left(\Delta_n^*,\Delta_t^*\right)=\frac{\partial J_R\left(\Delta_n^*,\Delta_t^*\right)}{\partial\Delta_t^*}. \tag{2}$$

Thus, if the fracture resistance, J_R, the end-opening, Δ_n^* and the end-sliding, Δ_t^* are recorded during a series of mixed mode fracture experiments, the traction-separation laws can be obtained by partial differentiation. To do so, we need test specimen configurations for which the J integral can be obtained from external loads, preferably in closed analytical form.

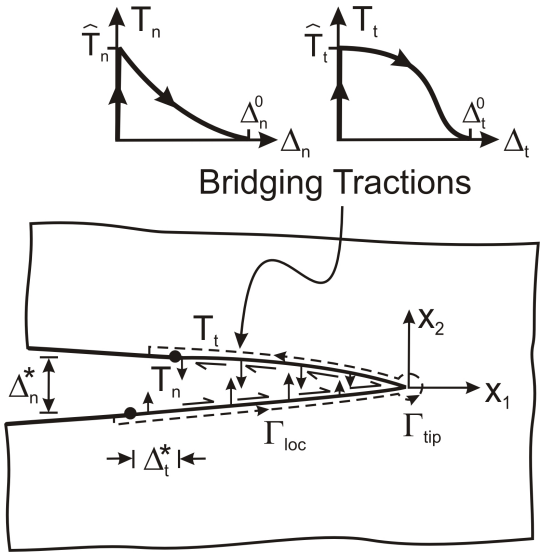

Figure 2. Schematics of a crack bridging problem.

3 J integral specimens

Fig. 3 shows a family of J integral fracture mechanics specimen. They are DCB (double cantilever beam) specimens consisting of slender beams loaded by bending moments and axial (but not transverse) forces. They share the common feature that the tractions along the external boundaries are normal stresses acting parallel to the cracking plane (the x_1-direction). Then an evaluation of the J integral along the external boundaries gives equations that are independent of the crack length and details of the traction-separation laws of the bridging zone.

Fig. 3a shows a pure Mode I specimen consisting of a symmetric DCB loaded by pure bending moments. Assume that the material is orthotropic with a symmetry plane parallel to the cracking plane (the x_1-direction). Then, the J integral evaluated around the external boundaries gives under plane stress conditions [2]

$$J_{ext}=\frac{12M^2}{B^2H^3E_{11}}, \tag{3}$$

where M is the applied bending moment applied to the beam-ends, B is the specimen width, H is the beam thickness, E_{11} is the Young's modulus of the beam in the x_1-direction.

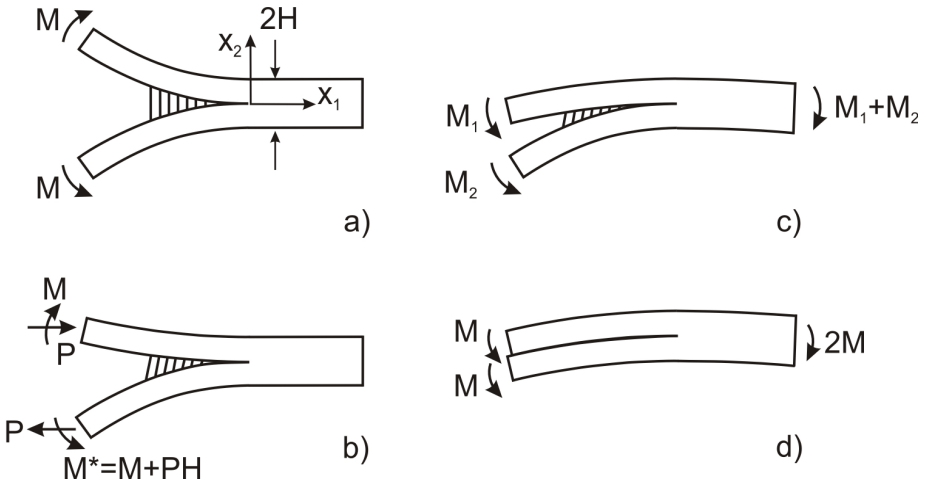

Figure 3. Family of J integral fracture specimens: (a) DCB specimen loaded with pure bending moments (Mode I), (b) DCB specimen loaded with axial forces and bending moments (mixed mode), (c) DCB specimen loaded with uneven bending moments (mixed mode) and (d) DCB specimen loaded with identical moments (Mode II).

Fig. 3b shows a DCB specimen loaded with a combination of axial force, P, and a bending moment, M. The J integral result for this specimen configuration is (plane stress) [11]:

$$J_{ext} = \frac{7P^2H^2 + 12M^2 + 12PHM}{B^2H^3E_{11}}. \tag{4}$$

This is a mixed mode specimen. Mode I is obtained for $P = 0$ and Mode II is obtained for $M/PH = -1/2$.

Another mixed mode specimen configuration is shown in Fig. 3c. This is a DCB specimen loaded with uneven bending moments (DCB-UBM). The two bending moments, M_1 and M_2, are taken positive in the directions shown in the figure. The J integral evaluated around the external boundaries gives (plane stress) [12]:

$$J_{ext} = \frac{21\left(M_1^2 + M_2^2\right) - 6M_1M_2}{4B^2H^3E_{11}} \quad for \quad |M_1| \le M_2. \tag{5}$$

Pure Mode I (Fig. 3a) is recovered for $M_1/M_2 = -1$ and pure Mode II is obtained for $M_1/M_2 = 1$ (Fig. 3d). Then, the J integral result can be expressed as (plane stress):

$$J_{ext} = \frac{9M^2}{B^2H^3E_{11}}. \tag{6}$$

Note that since the equation for J for all specimen configurations are independent of the crack length, they will give stable crack growth, so that complete traction-separation laws can be obtained. Note also that the J integral equations only depend on a single orthotropic elastic parameter, the Young's modulus E_{11}. The J integral results, Eqs. (3) - (6), are all independent

of the other orthotropic elastic parameters (the Young's modulus in the x_2-direction, the in-plane shear modulus and the two Poisson's ratios).
In summary, the test specimen configurations shown in Fig. 3 all have J integral equations that depends only on applied load (moments and axial forces), a Young's modulus of the test material and the specimen dimensions. Conduction fracture mechanics experiments using these J integral specimens enable the calculation of the fracture resistance, J_R directly using eq. (3) - (6). Furthermore, if the end-opening, Δ_n^* and the end-sliding, Δ_t^* are recorded during a series of mixed mode experiments, mixed mode traction-separation laws can be obtained by the procedure described above, i.e., by the use of eq. (2). This procedure only involves the fitting of J_R as a function of Δ_n^* and Δ_t^* and performing partial differentiation. No further numerical simulations of the test specimen are required. No a priory knowledge or assumption is made regarding the specific shape or coupling of the mixed mode traction-separation laws.
Examples of practical design of test device for the proposed J integral fracture specimen configurations of Fig. 3 can be found in the literature. The DCB loaded by pure bending moments (Fig. 3a) has been developed [13, 14]. The DCB loaded a combination of an axial force and a bending moment (Fig. 3b) is developed for testing in a scanning electron microscope [15]. Slightly different test configurations for the DCB-UBM were used by in studies of mixed mode cracking of adhesive joints [16, 17]. Determination of mixed mode traction-separation laws by the J integral approach has been demonstrated [18].

4 Discussion

4.1 Difference between J integral and energy release rate equations

For LSB problems, $J_{ext} \neq \mathcal{G}$ (with $\mathcal{G}$ being the LEFM potential energy release rate) for most fracture mechanics test specimen configurations [3]. Then, LEFM solutions for $\mathcal{G}$ or stress intensity factors are not directly applicable for LSB problems. To illustrate the difference, consider the standard Mode I DCB-specimen loaded with transverse force. An accurate calibration of the energy release rate is given by [19]

$$\mathcal{G} = \frac{12 P^2 a^2}{B^2 H^3 E_{11}} \left(1 + 0.677\, H/a\right)^2, \tag{7}$$

where the second term in the right hand side parenthesis accounts for the so-called root root rotation [20]. For long cracks, $a >> H$, eq. (7) approaches

$$\mathcal{G} = \frac{12 P^2 a^2}{B^2 H^3 E_{11}}, \tag{8}$$

which is the results that can be obtained e.g. by the compliance method modeling the cantilever beams using the ordinary, simple Bernoulli-Euler beam theory.
The J integral solution for the DCB specimen loaded with wedge forces is [21]

$$J_{ext} = \frac{2P\theta}{B}, \tag{9}$$

where P denotes the applied transverse force and θ is the rotation of the beam at the point where the transverse for is applied, see Fig. 4. Eq. (9) applies for both LSB and for small-

scale fracture process zone, i.e., LEFM conditions. Consider first crack growth under LEFM conditions for which $J_{ext} = \mathcal{G}$. From simple beam theory, the rotation angle can be estimated using a cantilever beam that is built-in at one end and loaded with the transverse force at the other end (this approach will underestimate the beam rotation of the DCB specimen since the beam model assumes no rotation at the build-in end, i.e., neglects the root rotation). The result obtained from a standard hand book of beam-theory is

$$\theta = \frac{6Pa^2}{BH^3 E_{11}}. \tag{10}$$

Inserting Eq. (10) into Eq. (9) recovers - as expected - the LEFM solution for long cracks, Eq. (8). Consider next the effect of LSB. Observe that, as shown in Fig. 4, the normal tractions in the bridging zone restrain the beam deflection and reduces the rotation of the beam-end, θ, and thereby reduces (by (9)) the J integral value. Consequently, the value of J of a DCB specimen having LSB is less than the LEFM energy release rate result, Eq. (7), $J_{ext} < \mathcal{G}$. Thus, in case the LEFM result is used for the calculation of fracture resistance for LSB problems, the fracture resistance will be overestimated. This overestimation can be significant [2]. Since the precise value of θ (and thus J_{ext}) depends on the details of the traction-separation laws, J_{ext} cannot be determined in closed analytical form for a DCB specimen loaded with transverse force. An experimental determination of J_{ext} for LSB problems requires the measurement of θ; this has been made by Stigh and co-workers using a shaft-encoder [22]. Measurements of rotations are also required for mixed mode specimen loaded with transverse forces, such as the mixed mode bending specimen (MMB) developed by Reeders and Crews [23] and the mixed mode double cantilever beam (MCB) specimen of Högberg and Stigh [24]; a J integral determination require the measurement of two independent rotation of the two beams. This has been accomplished experimentally by the use of digital image correlation [25].

4.2 The concept of steady-state cracking

The proposed J integral fracture mechanics test configuration has another attractive feature: They enable crack growth in steady-state. In order to clarify this, we will briefly explain the concept of steady-state cracking. When the end-opening reached the critical separation ($\Delta_n^* = \Delta_n^0$ for pure Mode I), the bridging zone is said to be fully developed. With further crack extension, the fracture resistance remains at the same, steady-state value, J_{ss}. However, this does not necessary imply that the cracking occurs in a self-similar fashion. For the standard DCB specimen loaded with wedge forces, the length of the fully-developed bridging zone, *L*, becomes shorter with increasing crack length [2]. This occurs because the beam curvature and deflection change as the crack length increases. As illustrated in Fig. 4, the beam experiences the largest curvature (and largest bending moment) at the crack tip, decreasing along the length of the specimen, approaching zero curvature at the point of application of the transverse forces.

In contrast, for the proposed DCB specimen loaded with axial forces and bending moments (Fig. 3), the specimens retain the same curvature when the bridging zone is fully-developed. As a result, a fully-developed fracture process zone translates along the specimen in a self-similar fashion under LSB. This is denoted steady-state cracking. Large-scale steady-state cracking is unique to slender beams [2]. One important implication of steady-state cracking is that all bridging ligaments will undergo the same opening-history since the steady-state bridging zone length, L_{ss}, remains the same for a fully-developed bridging zone. With all

ligaments undergoing the same cyclic opening history, it is anticipated that the steady-state specimen of Fig. 3 are better suited for the study of cyclic crack growth involving LSB.

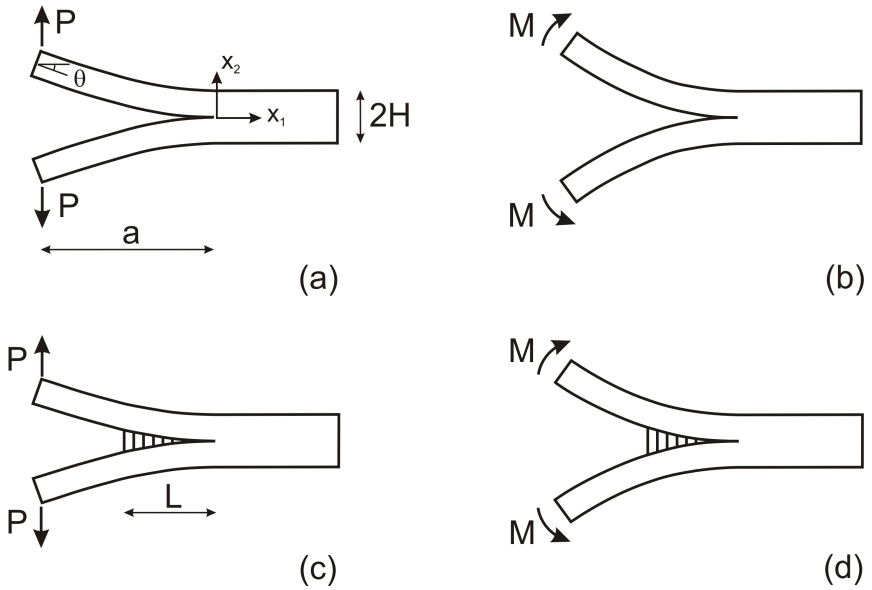

Figure 4. Illustration of deflection and rotation of unbridged and bridged specimens.

5 Conclusions

A family of DCB specimens loaded with axial forces and bending moments are proposed for fracture mechanical characterization of fracture problems that involves large-scale bridging. These specimens can be used in connection with a J integral approach for the determination of traction-separation laws in a fairly standard manner. As such, they can be considered as being a new generation of fracture specimens suitable for large-scale bridging problems, while most standard linear elastic fracture mechanics test specimens are restricted to be used for small-scale bridging (linear elastic fracture mechanics) problems.

Acknowledgements

This work was partially supported by the Danish Centre for Composite Structures and Materials for Wind Turbines (DCCSM), grant no. 09-067212 from the Danish Strategic Research Council.

References

[1] Albertsen H., Ivens J., Peters P., Wevers M., Verpost I. Interlaminar fracture toughness of CFRP influenced by fibre surface treatment: part 1. Experimental results. *Composite Science Technology*, **54**, 133-45 (1995).

[2] Suo Z., Bao G., Fan B. Delamination R-curve phenomena due to damage. *J. Mech. Phys. Solids.*, **40**, pp. 1-16 (1992).

[3] Bao G., Suo Z. Remarks on crack-bridging concepts. *Applied Mech. Rev.,* **45**, pp. 355-61 (1992).

[4] Yang Q. D., Thouless M. D., Ward S. M. Numerical simulations of adhesively-bonded beams failing with extensive plastic deformation. *J. Mech. Phys. Solids*, **47**, pp. 1337-53 (1999).

[5] Mohammad I., Liechti K. M. Cohesive zone modelling of crack nucleation at bimaterial corner. *Journal of the Mechanics Physics of Solids*, **48**, pp. 735-64 (2000).
[6] Kafkalidis M. S., Thouless M. D. The effect of geometry material properties of the fracture of single lap-shear joints. *Int. J. Solids Structures*, **39**, pp. 4367-83 (2002).
[7] Tada H., Paris P. C., Irwin G. R. *The stress analysis of cracks hand book*, American Society of Mechanical Engineers (2000).
[8] Rice J. R. A path independent integral the approximate analysis of strain concentrations by notches cracks. *J. Appl. Mech.*, **35**, pp. 379-86 (1968).
[9] Li V. C., Ward R. J. A novel testing technique for post-peak tensile behaviour of cementitious materials. *Fracture toughness fracture energy - testing methods for concrete rocks* (eds. H. Mihashi, H. Takahashi F. H. Wittmann), A. A. Balkema Publishers, pp. 183-95, Rotterdam (1989).
[10] Sørensen B. F., Kirkegaard P. Determination of mixed mode cohesive laws. *Engineering Fracture Mechanics*, **73**, pp. 2642-61 (2006).
[11] Suo Z., Hutchinson J. W. Interface crack between two elastic layers. *Int. J. Fract.*, **43**, pp. 1-18 (1990).
[12] Sørensen B. F., Jørgensen K., Jacobsen T. K., Østergaard R. C. DCB-specimen loaded with uneven bending moments. *International Journal of Fracture*, **141**, pp. 159-172 (2006).
[13] Freiman S. W., Mulville D. R., Mast P. W. Crack propagation studies in brittle materials. *Journal of Materials Science*, **8**, pp. 1527-33 (1973).
[14] Sørensen B. F., Jacobsen T. K. Large scale bridging in composites: R-curve bridging laws. *Composites part A*, **29A**, pp. 1443-51 (1998).
[15] Sørensen B. F., Gamstedt E. K., Østergaard R. C., Goutianos S. Micromechanical model of cross-over fibre bridging - prediction of mixed mode bridging laws. *Mechanics of Materials*, **40**, pp. 220-34 (2008).
[16] Plausinis D., Spelt J. K. Application of a new constant G load-jig to creep crack growth in adhesive joints. *International Journal of Adhesion and Adhesives*, **15**, pp. 225-32 (1995).
[17] Sørensen B. F., Goutianos S., Jacobsen T. K. Strength scaling of adhesive joints in polymer-matrix composites. *International Journal of Solids Structures*, **46**, pp. 741-61 (2009).
[18] Sørensen B. F., Jacobsen T. K. Delamination of fibre composites: determination of mixed mode cohesive laws. *Composite Science Technology*, **69**, pp. 445-56 (2009).
[19] Wiederhorn S. M. Influence of water vapor on crack propagation in soda-lime glass. *J. Am. Ceram. Soc.*, **50**, pp. 407-14 (1967).
[20] Williams J.G. End correction for orthotropic DCB specimen. *Comp. Sci. Tech.*, **35**, 367–376 (1989).
[21] Paris A. J., Paris P. C. Instantaneous evaluation of J and C*. *Int. J. Fracture*, **38**, pp. R19-R21 (1988).
[22] Andersson T., Stigh U. The stress-elongation relation for an adhesive layer loaded in peel using equilibrium of energetic forces. *Int. J. Solids Structures*, **41**, 413–434 (2004).
[23] Reeder J. R., Crews Jr J. H. Redesign of the mixed-mode bending delamination testing. *Journal Of Composites Technology & Research*, **14**, pp. 12-19 (1992).
[24] Högberg J. L., Stigh U. Specimen proposals for mixed mode testing of adhesive layer. *Engineering Fracture Mechanics*. **73**, pp. 2541–87 (2006).
[25] Högberg J. L., Sørensen B. F., Stigh U. Constitutive behaviour of mixed mode loaded adhesive layer. *International Journal of Solids Structures*, **44**, pp. 8335-54 (2007).